

## A FLOW-CONDITION-BASED INTERPOLATION MIXED FINITE ELEMENT PROCEDURE FOR HIGHER REYNOLDS NUMBER FLUID FLOWS

KLAUS-JÜRGEN BATHE\* and JUAN P. PONTAZA

*Department of Mechanical Engineering, Massachusetts Institute of Technology,  
77 Massachusetts Avenue, Cambridge, MA 02139, USA*

*\*kjb@mit.edu*

Received 30 July 2001

Communicated by F. Brezzi

We present a (somewhat) new finite element procedure for the analysis of higher Reynolds number fluid flows. While two-dimensional conditions and incompressible fluid flows are considered, the scheme can directly be used for three-dimensional conditions and also has good potential for compressible flow analysis. The procedure is based on the use of a nine-node element, optimal for incompressible analysis (the 9/3 or 9/4-c elements), and a Petrov–Galerkin formulation with exponential weight functions (test functions). These functions are established from the flow conditions along the edge- and mid-lines of the element. An important feature is that for low Reynolds number flow, the weight functions are the usual biquadratics and as higher Reynolds number flow is considered, the functions “automatically” skew so as to provide the necessary stability for the solution (the upwinding effect). Since the test functions are calculated by the flow conditions, no artificial constant is set by the analyst. The procedure is simple to implement. We present some solution experiences and conclude that while the procedure is not the “ideal” solution scheme sought, it has some valuable attributes and good potential for further improvements.

*Keywords:* Finite elements; incompressible fluid flows.

AMS Subject Classification: 76D05, 35Q30, 65M60

### 1. Introduction

Much effort has been directed towards the development of efficient finite element methods for flow problems. However, to date, by far most fluid flow analyses are still being performed using finite difference and control volume based methods.<sup>1</sup> While it is generally recognized that finite element procedures have a strong mathematical basis, it has also been established that they are computationally not as efficient. However, largely low-order finite elements have been used.

In earlier research we explored whether parabolic finite elements can provide an efficient solution procedure. Parabolic elements are very efficient in structural analysis, the solution of field problems and they may also be effective in fluid flow

analyses. For this reason we tested various solution schemes using parabolic finite elements and reported on our results in an earlier paper.<sup>2</sup> The available schemes are very effective for low Reynolds number flow but no single procedure performed satisfactorily in high Reynolds number flow conditions. Hence, we concluded that more research is needed and major advances must still be sought.

When formulating the governing finite element equations for incompressible fluid flow, two key difficulties must be addressed: the incompressibility condition (the continuity equation) must be appropriately imposed and the convection term in the Navier–Stokes equations must be appropriately discretized. These two effects will cause numerical instabilities in the solution or prevent a solution altogether, if not properly represented in the finite element procedure.

As for the incompressibility condition, considering two-dimensional flows, the mixed-interpolated nine-node velocity-based elements with either a linear discontinuous pressure interpolation (the 9/3 element) or a bilinear continuous pressure interpolation (the 9/4-c element) are optimal,<sup>3</sup> and hence very attractive candidates for a general solution procedure. But it remains to develop an effective scheme for the elements to represent the convection term in the Navier–Stokes equations when high Reynolds number flow is considered.

Various finite element schemes to solve high Reynolds number fluid flows have been proposed, and among them streamline upwind Petrov–Galerkin procedures, and closely related techniques, have been extensively researched.<sup>1,2</sup> Test results using some of these methods and a higher-order derivative artificial diffusion method, all embedded in a nine-node element are given in Ref. 2, where, as stated above already, shortcomings of all these methods are demonstrated.

These shortcomings also include the fact that in the techniques some parameters need to be set to reach stability. These parameters appear rather artificial (to introduce the appropriate amount of artificial diffusion) but have been related to the calculation of bubbles in the elements.<sup>4</sup>

In Ref. 2, we also describe what we labeled to be an “ideal” solution scheme. Using this procedure, for a well-posed problem, a reasonable flow solution would always be obtained when using a reasonable mesh, even at high Reynolds numbers, and as the mesh is refined more details of the flow would be calculated. Here it is valuable to refer to some theoretical work, in which it was established that the Navier–Stokes equations are self-consistent up to about Reynolds number  $10^6$ , and that weak solutions of well-posed transient problems exist, of course subject to smooth boundary and initial conditions.<sup>5,6</sup> Therefore, it is reasonable to endeavor to obtain a finite element procedure that will solve high Reynolds number flows with the attributes of the “ideal” solution scheme although this is a difficult goal to reach.

Our objective in this paper is to present a finite-element solution scheme which is simple and a natural extension of a procedure known to be optimal for low Reynolds number flow solutions. Namely, we use a nine-node mixed interpolated velocity/pressure element (either the 9/3 or 9/4-c element) established using the

Galerkin procedure and simply change the weight, i.e. test, functions to correspond to the specific flow conditions encountered. We use exponential functions along the edges and mid-lines of the element evaluated from the flow conditions, and the tensor product of these functions for the interior of the element. The essence of the approach is therefore to capture the flow conditions *surrounding and within* the element in the weight functions. At a low Reynolds number, the weight functions collapse automatically to the biquadratic functions, but the weight functions naturally skew to the upstream side as the Reynolds number increases. The amount of skewing is determined by the Reynolds number and solved for by establishing the element edge- and mid-line functions. There is no artificial upwind parameter to be set and the flow conditions surrounding an element determine the equations used for the element.

In the following sections we first present the finite element procedure, then we discuss some basic considerations regarding the scheme and present some solution experiences. We finally mention that the proposed solution procedure needs much further study and development to get close to the “ideal” solution scheme, but that the approach has much potential for the solution of incompressible and compressible flows.

Throughout the paper, the usual notation for Sobolev spaces is used, see for instance Ref. 7.

## 2. The Flow-Condition-Based Interpolation Procedure

Let  $\Omega \in R^2$  be a bounded domain with boundary  $S$  and  $\mathbf{x} = (x_1, x_2)$  be a point in  $\Omega$ . We consider the solution of the Navier–Stokes equations governing incompressible flow, which in non-dimensionalized form can be written as:

Find the velocity  $\mathbf{v}(\mathbf{x}, t)$  and pressure  $p(\mathbf{x}, t)$  such that

$$\frac{\partial \mathbf{v}}{\partial t} + (\mathbf{v} \cdot \nabla)\mathbf{v} + \nabla p - \frac{1}{\text{Re}} \nabla^2 \mathbf{v} = 0 \quad \text{in } \Omega \times (0, \tau], \tag{1}$$

$$\nabla \cdot \mathbf{v} = 0 \quad \text{in } \Omega \times (0, \tau], \tag{2}$$

$$\mathbf{v}(\mathbf{x}, 0) = {}^0\mathbf{v}(\mathbf{x}) \quad \text{in } \Omega, \tag{3}$$

$$\mathbf{v} = \mathbf{v}^s \quad \text{on } S_v, \tag{4}$$

$$\tilde{\boldsymbol{\sigma}} \cdot \mathbf{n} = \tilde{\mathbf{f}}^s \quad \text{on } S_f, \tag{5}$$

where  $S = S_v \cup S_f$  and  $S_v \cap S_f = \emptyset$ ,  $\tau$  is a real number (time)  $> 0$ ,  $\text{Re}$  is the Reynolds number,  $\tilde{\boldsymbol{\sigma}}$  is a pseudo-stress,  $\tilde{\boldsymbol{\sigma}} = -p\mathbf{I} + (1/\text{Re})\nabla\mathbf{v}$ ,  $\mathbf{n}$  is the unit normal to the boundary of  $\Omega$ ,  $\mathbf{v}^s$  is the prescribed velocity on the boundary  $S_v$ ,  $\tilde{\mathbf{f}}^s$  are the prescribed pseudo-tractions on the boundary  $S_f$ , and in Eq. (3) the initial conditions are given. We assume that the problem is well-posed. We use this form of the Navier–Stokes equations in this paper because the boundary conditions in Eq. (5) directly model outflow boundary conditions<sup>3</sup> as we have in our test problems in Sec. 4.

The variational form of these equations using the Petrov–Galerkin formulation is:

Find  $\mathbf{v} \in V$ ,  $\mathbf{v}(\mathbf{x}, 0) = {}^0\mathbf{v}(\mathbf{x})$ ,  $p \in Q$  such that for all  $\mathbf{w} \in W$  and  $q \in Q$

$$\int_{\Omega} \left[ \frac{\partial \mathbf{v}}{\partial t} + (\mathbf{v} \cdot \nabla) \mathbf{v} \right] \cdot \mathbf{w} d\Omega - \int_{\Omega} p(\nabla \cdot \mathbf{w}) d\Omega + \frac{1}{\text{Re}} \int_{\Omega} \nabla \mathbf{v} \cdot \nabla \mathbf{w} d\Omega = \int_{S_f} \tilde{\mathbf{f}}^S \cdot \mathbf{w} dS_f, \quad (6)$$

$$\int_{\Omega} (\nabla \cdot \mathbf{v}) q d\Omega = 0, \quad (7)$$

where we use the linear spaces<sup>a</sup>

$$V = \{ \mathbf{v} \in \mathbf{H}^1(\Omega), \mathbf{v}|_{S_v} = \mathbf{v}^s \},$$

$$W = \{ \mathbf{w} \in \mathbf{H}^1(\Omega), \mathbf{w}|_{S_v} = 0 \},$$

$$Q = \{ q \in H^0(\Omega); \text{ or } q \in H^1(\Omega) \}.$$

We note that if the same functions are used in  $W$  as in  $V$ , the variational formulation corresponds to the standard Galerkin method (the Bubnov–Galerkin method). However, we use a more general approach and therefore will in general not have that  $W$  and  $V$  coincide (when  $\mathbf{v}^s = 0$ ).

For the finite element solution we choose subspaces  $V_h$ ,  $W_h$ , and  $Q_h$  of the infinite-dimensional spaces  $V$ ,  $W$  and  $Q$ , respectively. The finite element solution procedure is then:

Find  $\mathbf{v}_h \in V_h$ ,  $\mathbf{v}_h(\mathbf{x}, 0) = {}^0\mathbf{v}(\mathbf{x})$ ,  $p_h \in Q_h$  such that for all  $\mathbf{w}_h \in W_h$  and  $q_h \in Q_h$

$$\begin{aligned} & \int_{\Omega} \left[ \frac{\partial \mathbf{v}_h}{\partial t} + (\mathbf{v}_h \cdot \nabla) \mathbf{v}_h \right] \cdot \mathbf{w}_h d\Omega - \int_{\Omega} p_h (\nabla \cdot \mathbf{w}_h) d\Omega + \frac{1}{\text{Re}} \int_{\Omega} \nabla \mathbf{v}_h \cdot \nabla \mathbf{w}_h d\Omega \\ & = \int_{S_f} \tilde{\mathbf{f}}^S \cdot \mathbf{w}_h dS_f, \end{aligned} \quad (8)$$

$$\int_{\Omega} (\nabla \cdot \mathbf{v}_h) q_h d\Omega = 0. \quad (9)$$

The key to reaching an effective solution scheme lies of course in choosing appropriate finite element spaces. We use the following spaces: for the solution space  $V_h$  we use continuous biquadratic functions, for the solution space  $Q_h$  we use linear discontinuous or bilinear continuous functions, giving essentially the same results, and for the test function space  $W_h$  we use exponential functions. An element of the new space  $W_h$  is established as follows.

Figure 1 shows a typical nine-node undistorted rectangular element. To include the effect of element distortions, the usual transformations of isoparametric elements can be used.<sup>3</sup> Based on the knowledge that at high Reynolds (or Péclet) number flows the solution contains exponential functions, we assume the following functions

<sup>a</sup>Actually, to be precise,  $V$  is not a linear space but an affine manifold (the same holds for the finite element space  $V_h$  used later).

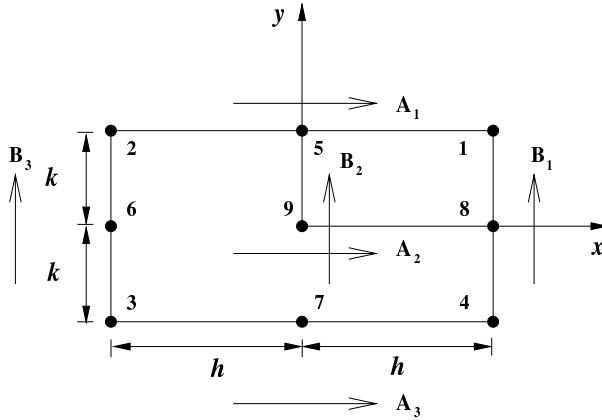


Fig. 1. Typical nine-node rectangular element.

along the edge- and mid-lines of the element: for the three functions along lines 2-5-1, 6-9-8 and 3-7-4 in the variable  $x$

$$\phi_i(x) = a_i(e^{-2A_i x} - 1) + b_i x + c_i, \quad i = 1, 2, 3 \tag{10}$$

for the three functions along lines 4-8-1, 7-9-5 and 3-6-2 in the variable  $y$

$$\phi_i(y) = d_i(e^{-2B_i y} - 1) + e_i y + f_i, \quad i = 1, 2, 3 \tag{11}$$

where for each  $i$

$$2A = \text{Re } v_1 \quad 2B = \text{Re } v_2, \tag{12}$$

$v_1$  and  $v_2$  are representative velocities along the lines considered (we used the velocities at the mid-nodes) and the constants are determined using the conditions at the nodes. Normalizing these functions to have the Kronecker delta property at the nodes, we obtain along an edge or mid-line, e.g. in the  $x$ -direction, the three generic interpolation functions

$$h_1(x) = \frac{(e^{-2Ax} - 1)}{4 \sinh^2 Ah} - \frac{x}{2h} + \frac{x}{2h} \coth Ah, \tag{13}$$

$$h_2(x) = -\frac{2(e^{-2Ax} - 1)}{4 \sinh^2 Ah} - \frac{x}{h} \coth Ah + 1, \tag{14}$$

$$h_3(x) = \frac{(e^{-2Ax} - 1)}{4 \sinh^2 Ah} + \frac{x}{2h} + \frac{x}{2h} \coth Ah. \tag{15}$$

Figure 2 shows the functions for the element Reynolds numbers  $10^{-5}$ , 10 and 100. Note that for very small Reynolds numbers these interpolations are the usual parabolic functions and that as the element Reynolds number increases the functions skew to the upstream side.

An element of  $W_h$  is now obtained by simply interpolating the edge- and mid-line functions quadratically over the element and then taking the tensor product of

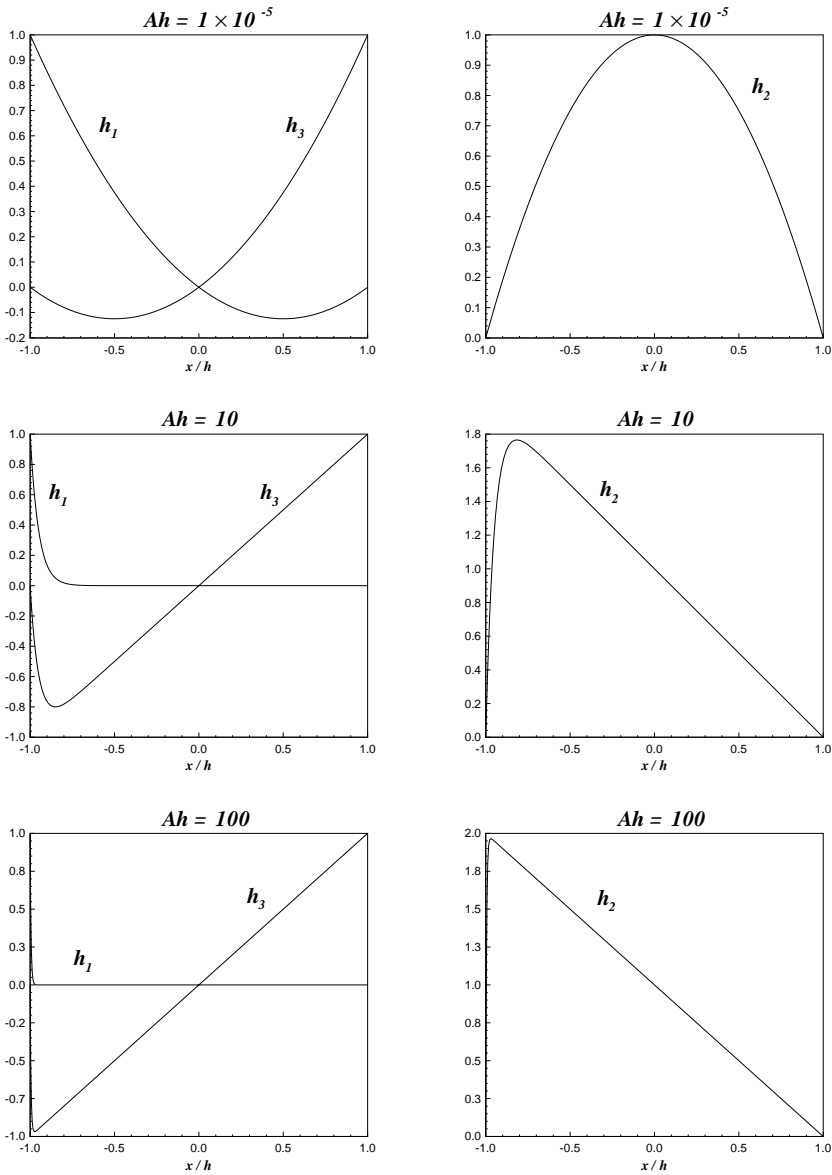


Fig. 2. Element edge test functions.

these interpolations. Consider the two nine-node element patch in Figs. 3a and 4a. In the case of pure diffusion, the test functions of nodes A and B are symmetric, see Figs. 3b and 4b. Figures 3c and 4c show the test functions when convection is present, for the case of uniform flow in the positive  $x$  direction. Figures 3d and 4d show the functions for the case of uniform flow at an angle, both  $x$  and  $y$  components of velocity are present.

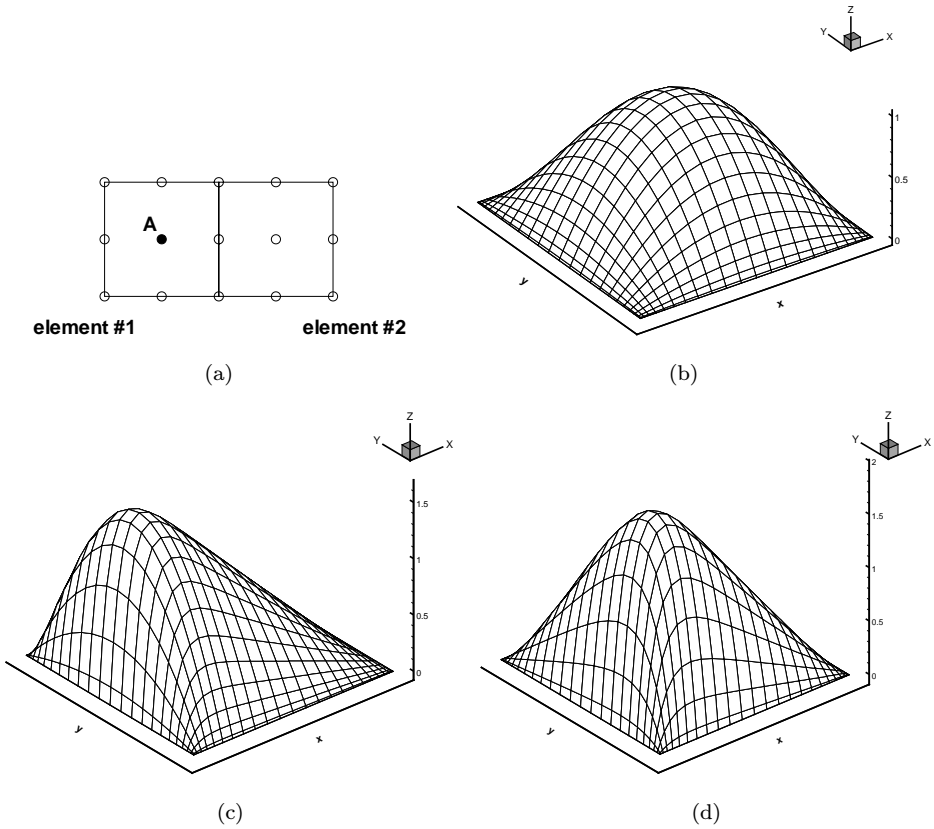


Fig. 3. Test function for node A in the two-element patch in (a). In the case of pure diffusion the test function is symmetric (b). In (c) convection is present, flow is strictly in the positive  $x$  direction. In (d) convection is present in the positive  $x$  and  $y$  directions, flow at a  $30^\circ$  angle from the  $x$ -axis.

### 3. Some Basic Considerations

A number of important considerations need to be addressed for the implementation and use of the element.

#### 3.1. Numerical integration

An important part of the evaluation of the finite element matrices is the numerical integration used. For low Reynolds number flow solutions,  $3 \times 3$  Gauss integration corresponds to “full” numerical integration. This integration does not evaluate the exact finite element matrices when the element is distorted but the error is acceptable provided reasonable distortions are considered.<sup>3</sup>

For higher Reynolds number flow, the test functions are more complicated and a higher-order integration scheme is needed. The required order is clearly dependent on the element Reynolds number. For the moment, we are using the following

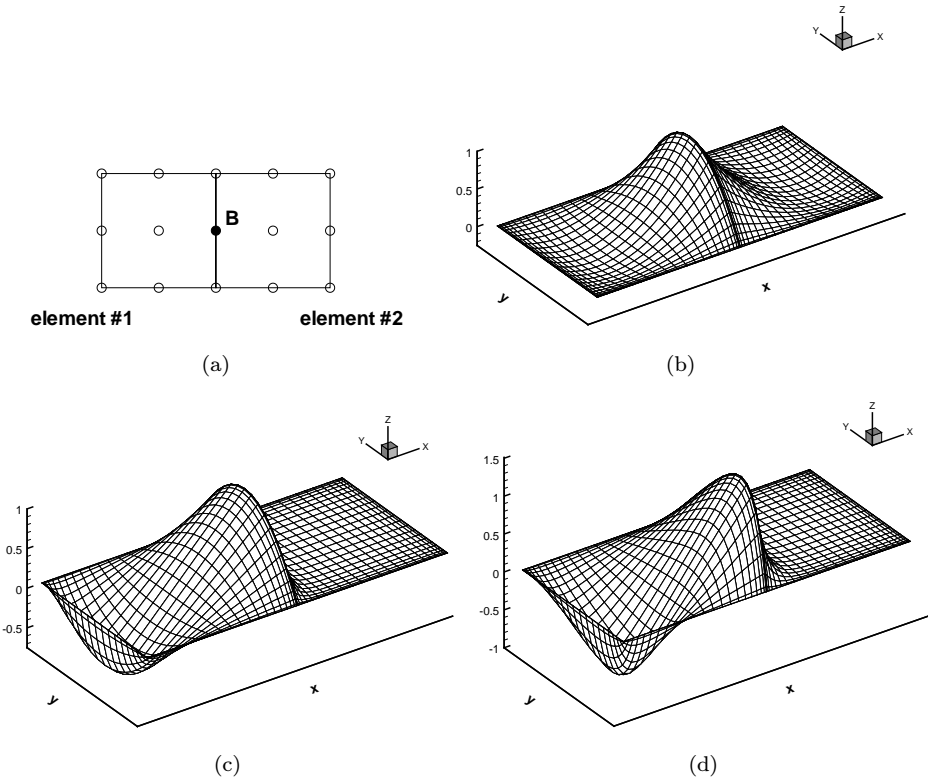


Fig. 4. Test function for node B in the two-element patch in (a). In the case of pure diffusion the test function is symmetric (b). In (c) convection is present, flow is strictly in the positive  $x$  direction. In (d) convection is present in the positive  $x$  and  $y$  directions, flow at a  $30^\circ$  angle from the  $x$ -axis.

formula for the Gauss integration order used:

$$\text{Integration Order} = \begin{cases} 3 \times 3 & \text{if } 10^{-6} \leq \max(|Ah|, |Bk|) \leq 2.5 \\ 5 \times 5 & \text{if } 2.5 < \max(|Ah|, |Bk|) \leq 5.0 \\ 7 \times 7 & \text{if } \max(|Ah|, |Bk|) > 5.0 \end{cases} \quad (16)$$

Hence the maximum integration order used is  $7 \times 7$  Gauss integration. Using this formula the element matrices do not exhibit any spurious eigenvalues.

While it may appear that the integration order used requires a considerable computational effort, it should be recognized that in flow simulations frequently over 90% of the solution effort pertains to the solution of the algebraic equations. Hence, although the effort for the element matrix evaluations increases significantly for the proposed scheme when higher Reynolds number flow is solved, this increase is not significant when measured on the total solution time required.

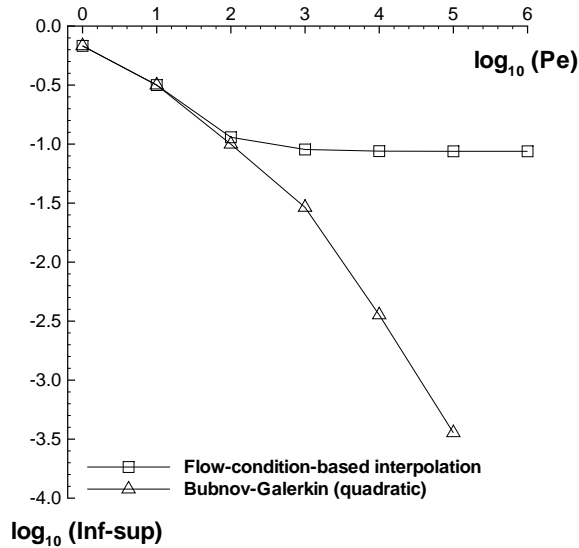


Fig. 5. Inf-sup test results for the one-dimensional high Péclet number flow problem.<sup>9</sup> The convection-diffusion problem corresponds to a constant prescribed velocity throughout the domain and prescribed temperatures at both ends of the domain. Sixteen equal size elements are used.

### 3.2. Stability

We mentioned already that two sources of instabilities can arise in a fluid flow solution scheme; the first regarding the incompressibility condition and the second regarding the representation of the convection term. A mathematical analysis of the discretization scheme presented in the previous section still needs to be performed, but we can already make the observation that the relevant inf-sup conditions should be satisfied in order to have a reliable scheme.<sup>3,8,9</sup>

Considering the incompressibility condition and low Reynolds number flow, the selected elements are stable and indeed optimal. The relevant inf-sup condition has been proven analytically to be satisfied. Considering the effect of the convection term, we have performed the inf-sup test of Ref. 9. The results of the test are given in Fig. 5, where the same test data as in Ref. 9 have been used. It is seen that the inf-sup test is passed by the scheme. Of course, this numerical test has only limited value, but the fact that the test is passed is encouraging to proceed with mathematical and convergence analyses.

### 3.3. A family of elements

The nine-node element presented here is a good candidate for the analysis of flow problems. However, the same approach of formulation can of course also be used to develop other elements, in fact a family of elements can be proposed. In each case, the element when used for Stokes flow solutions, should ideally satisfy the inf-sup condition for incompressible analysis.

With this in mind, the following elements can, for example, be considered:

- The four-node element presented in Ref. 10 with the  $\phi$  edge-line functions of the form

$$\phi(x) = a(e^{-2Ax} - 1) + b.$$

This element satisfies the inf-sup test for incompressible analysis; however, a simpler element is the 4/1 element (four nodes for velocities and a constant pressure assumption, which however does not satisfy the inf-sup condition for incompressible analysis).<sup>3</sup>

- The cubic quadrilateral elements with 16 nodes for the velocity and a quadratic discontinuous interpolation for pressure (the 16/6 element) or a biquadratic continuous interpolation for pressure (the 16/9-c element).<sup>3</sup> Appropriate  $\phi$  edge- and mid-line functions would then be

$$\phi(x) = a(e^{-2Ax} - 1) + bx^2 + cx + d.$$

And of course, additional quadrilateral and triangular elements can be established using the same approach.

### 3.4. *Use of conservative form of Navier–Stokes equations*

The presentation of the solution scheme was given using Eqs. (1) to (5) as the basic equations to be solved. In practice, we would actually discretize the conservative form of the Navier–Stokes equations in order to more closely satisfy continuity and momentum conservation. This requires, of course, that for each finite element the sum of the weight functions be equal to unity. Then, at the nodal point level, the two basic conditions of “nodal point flux equilibrium” and “element flux equilibrium” are satisfied, respectively, for the finite element assemblage and for each finite element in the assemblage (see p. 177 of Ref. 3). The interpolation functions used here satisfy this requirement.

## 4. Sample Solutions

In the absence of a deep theoretical analysis of the discretization scheme, it is important to solve well-chosen test problems. We proposed some problems in Ref. 2, which we use here in a sometimes strengthened form with the nine node element discussed above. The new solution procedure is referred to as an FCBI (Flow-Condition-Based Interpolation) scheme.

### 4.1. *Lid-driven cavity flow*

The lid-driven cavity flow problem has been used extensively as a test problem because of its complex flow physics and simple geometry. The presence of several recirculating regions makes this an interesting and challenging problem. We perform

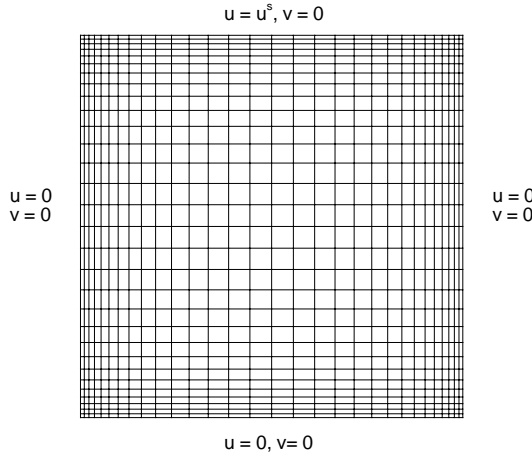


Fig. 6. Mesh and boundary conditions.

a steady state analysis for Reynolds numbers up to  $1 \times 10^4$ . A unit square with the non-uniform  $(30 \times 30)$ -element mesh, shown in Fig. 6, is used for the computations. In Fig. 7, we compare the horizontal velocity profiles at the vertical mid-section of the cavity obtained using the FCBI scheme with the benchmark solutions of Ghia *et al.*<sup>11</sup>

**4.2. Flow in a hundred-eighty degree bend**

The fluid flow in a bend of outer diameter of 21 and an inner diameter of 19 is considered. A parabolic velocity profile is specified at the inlet, zero pseudo-tractions at the outlet, and zero velocities at the walls. A  $(15 \times 150)$ -element mesh is used for the solutions; the mesh is non-uniform along the width and uniform along the length of the bend. Figure 8 shows the geometry and a partial view of the mesh.

The steady-state analysis results for Reynolds numbers up to  $1 \times 10^4$  are shown in Fig. 9. The pressure distributions along the outer and inner walls are compared with the results obtained using the classic Bubnov–Galerkin formulation. No solution was obtained with the Bubnov–Galerkin formulation for  $Re > 1 \times 10^3$ .

**4.3. Flow in an S-duct**

The flow in the S-duct shown in Fig. 10 is considered. The geometry, mesh and boundary conditions are shown in the figure. A parabolic profile of horizontal velocity is prescribed at the inlet. This is a difficult test problem and was considered in Ref. 2.

Figures 11 and 12 show the steady state velocity vector and pressure fields computed using the FCBI scheme for  $Re = 1 \times 10^2$  and  $Re = 1 \times 10^3$ , respectively.

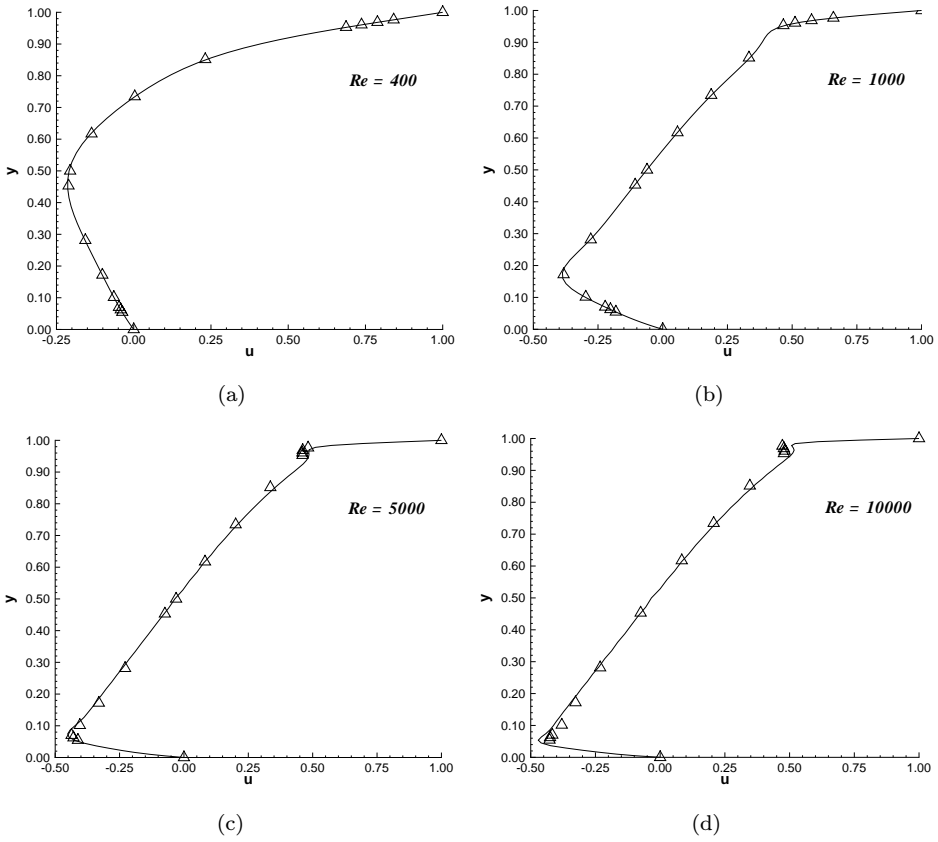


Fig. 7. Horizontal velocity profiles along the vertical mid-section of the cavity: — FCBI scheme,  $\triangle$  Ghia *et al.*<sup>11</sup>

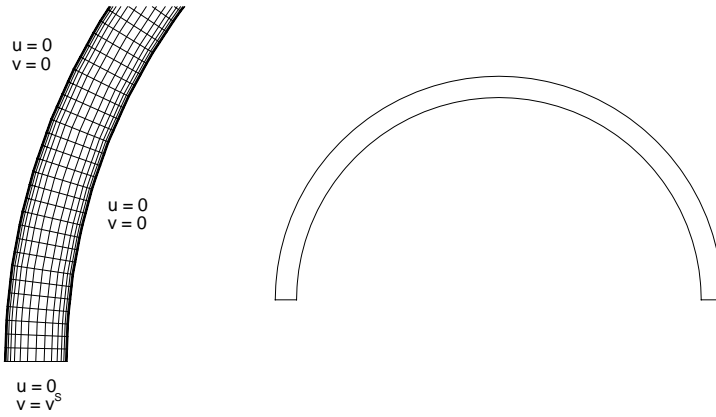


Fig. 8. Bend geometry and partial view of the mesh.

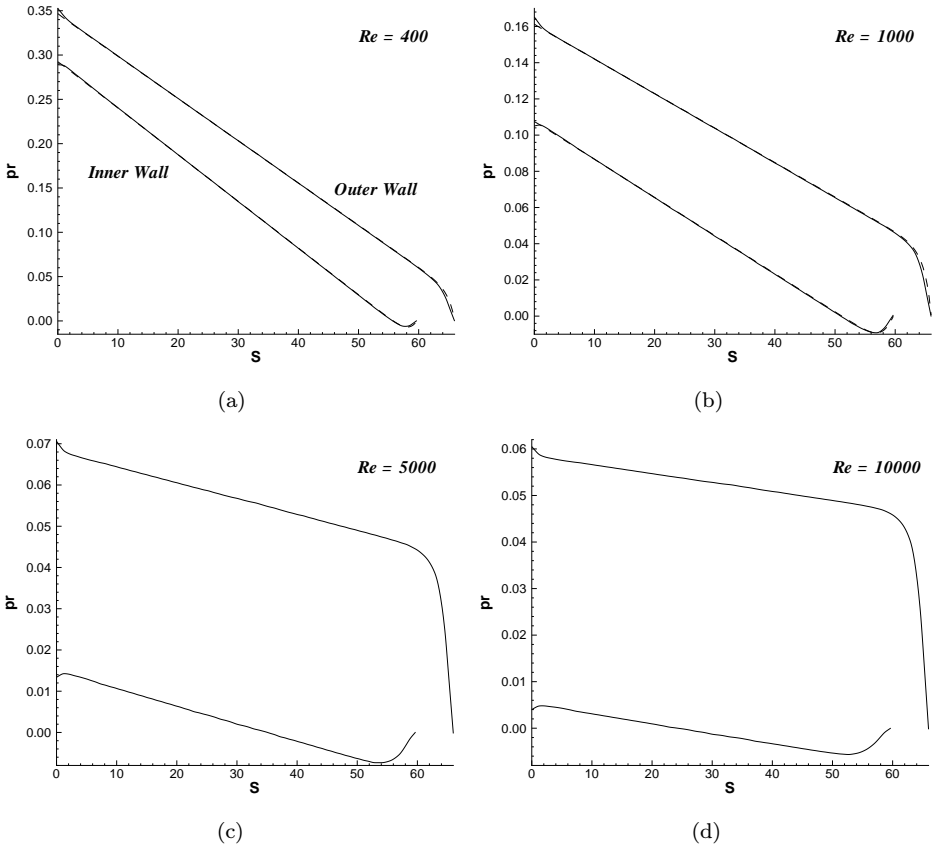


Fig. 9. Pressure profiles for the  $180^\circ$  bend flow: — FCBI scheme, --- Bubov-Galerkin formulation.

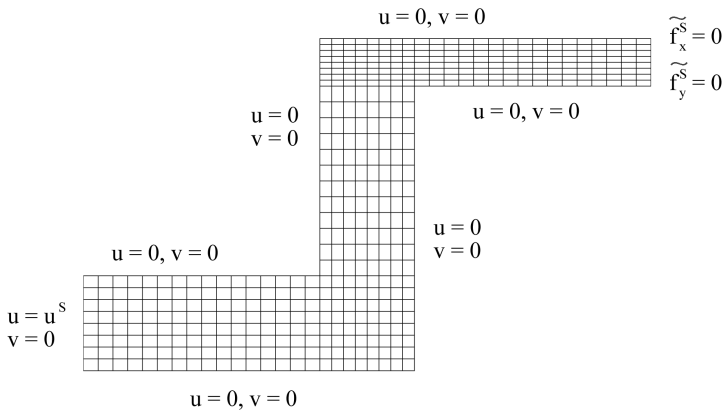


Fig. 10. Geometry, mesh and boundary conditions.

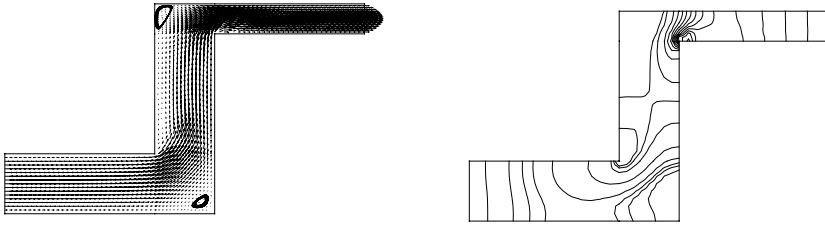


Fig. 11. Vector velocity field and pressure contours computed using the FCBI scheme for  $Re = 1 \times 10^2$ .

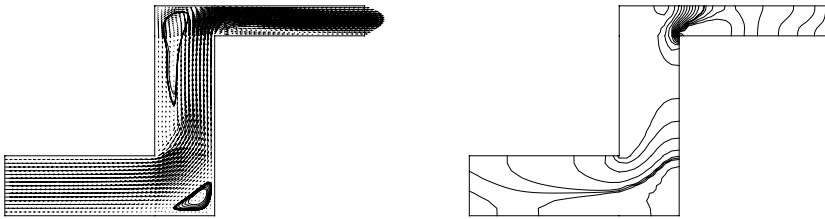


Fig. 12. Vector velocity field and pressure contours computed using the FCBI scheme for  $Re = 1 \times 10^3$ .

## 5. Concluding Remarks

In our research to obtain a finite-element solution scheme closer to the ideal scheme of Ref. 2 for high Reynolds number fluid flows, we have developed the finite element procedure presented in this paper. The procedure is simple and a natural extension of a discretization scheme known to be optimal for low Reynolds number flows. The scheme passed the numerical inf-sup test considering one-dimensional flow and has shown good accuracy in the solution of some test problems, but needs, of course, much further study and development.

The procedure given in the paper does not fulfill the requirements of the “ideal” solution scheme — a difficult goal to reach — described in Ref. 2. However, the approach used has further potential. The use of the given functions but aligned with the streamlines could be more effective. A more accurate analytical solution of the advective response *within* the element to construct the test functions could improve the procedure. Also, the use of trial functions reflecting the flow conditions can be explored. This approach has been pursued in Ref. 12.

The proposed scheme is clearly related to the use of residual-free bubbles, but the distinctive difference is that the procedure incorporates flow conditions on the element edges.<sup>13</sup> This feature is deemed important to reach an effective solution scheme.

While we considered in this paper only the use of a parabolic quadrilateral element, we indicated that this element is really a member of a family of quadrilateral and triangular elements all formulated using the approach given in the paper. Also,

the use of a parabolic element might be effective for compressible flow solutions<sup>14</sup> which indicates that for compressible flows the approach of this paper might be valuable as well.

## References

1. K. J. Bathe (ed.), *Computational Fluid and Solid Mechanics* (Elsevier, 2001).
2. D. Hendriana and K. J. Bathe, *On upwind methods for parabolic finite elements in incompressible flows*, *Int. J. Numer. Meth. Engrg.* **47** (2000) 317–340.
3. K. J. Bathe, *Finite Element Procedures* (Prentice Hall, 1996).
4. F. Brezzi, L. D. Marini and A. Russo, *Applications of the pseudo residual-free bubbles to the stabilization of convection–diffusion problems*, *Comput. Methods Appl. Mech. Engrg.* **166** (1998) 51–63.
5. C. R. Doering and J. D. Gibbon, *Applied Analysis of the Navier–Stokes Equations* (Cambridge Univ. Press, 1995).
6. A. Rauh, *Remarks on unsolved basic problems of the Navier–Stokes equations*, *Proc. of the Conf. Let's Face Chaos through Nonlinear Dynamics*, Maribor, Slovenia, June 24–July 5, 1996.
7. J. L. Lions and E. Magenes, *Nonhomogeneous Boundary Value Problems and Applications* (Springer-Verlag, 1972), Vol. 1.
8. K. J. Bathe, *The inf–sup condition and its evaluation for mixed finite element methods*, *Computers and Structures* **79** (2001) 243–252; 971.
9. K. J. Bathe, D. Hendriana, F. Brezzi and G. Sangalli, *Inf–sup testing of upwind methods*, *Int. J. Numer. Meth. Engrg.* **48** (2000) 745–760.
10. D. Pantuso and K. J. Bathe, *A four-node quadrilateral mixed-interpolated element for solids and fluids*, *Math. Models Methods Appl. Sci.* **5** (1995) 1113–1128.
11. U. Ghia, K. N. Ghia and C. T. Shin, *High-Re solutions for incompressible flow using the Navier–Stokes equations and the multigrid method*, *J. Comput. Phys.* **48** (1982) 387–411.
12. K. J. Bathe and H. Zhang, *A flow-condition-based interpolation finite element procedure for incompressible fluid flows*, *Computers & Structures*, in press.
13. F. Brezzi and L. D. Marini, *Subgrid phenomena and numerical schemes*, *Proc. Int. Symp. on Mathematical Modeling and Numerical Simulation in Continuum Mechanics*, Yamaguchi, September 29–October 3, 2000.
14. D. Hendriana and K. J. Bathe, *On a parabolic quadrilateral finite element for compressible flows*, *Comput. Methods Appl. Mech. Engrg.* **186** (2000) 1–22.